Experimental analysis of the optical gain and linewidth enhancement factor of GaInNAs/GaAs lasers

2004 J. Phys.: Condens. Matter 16 S3095

(http://iopscience.iop.org/0953-8984/16/31/007)

INSTITUTE OF PHYSICS PUBLISHING JOURNAL OF PHYSICS: CONDENSED MATTER

J. Phys.: Condens. Matter **16** (2004) S3095–S3106 PII: S0953-8984(04)74362-3

Experimental analysis of the optical gain and linewidth enhancement factor of GaInNAs/GaAs lasers

N C Gerhardt and M R Hofmann

Optoelektronische Bauelemente und Werkstoffe, Ruhr-Universität Bochum, Gebäude IC2/155, 44780 Bochum, Germany

E-mail: Nils.Gerhardt@ruhr-uni-bochum.de

Received 23 December 2003
Published 23 July 2004
Online at stacks.iop.org/JPhysCM/16/S3095
doi:10.1088/0953-8984/16/31/007

Abstract

The gain and α-factor spectra of a molecular-beam-epitaxy-grown 1.3 μm GaInNAs laser are experimentally determined using the method of Hakki and Paoli and a transmission method. The gain in our structure is due to inhomogeneously broadened band–band transitions but, in general, critically depends on the growth process. The value 2.5 for α at the laser emission wavelength clamps with increasing injection current.

1. Introduction

Growing bandwidth requirements for optical fibre communication demand long wavelength semiconductor lasers emitting in the 1.3 and 1.55 μm wavelength region. While GaInPAs/InP is a well established material system for edge emitting lasers in these wavelength regimes [1], its use in vertical-cavity surface emitting lasers (VCSELs) introduces considerable problems. The main difficulty is the lack of high quality Bragg reflectors that could be epitaxially grown lattice matched on InP substrate. However, VCSELs are superior to edge emitting lasers for applications in telecommunications because of their numerous advantages with regard to optical fibre coupling and dynamical single-mode operation. New GaAs-based material systems based on dilute nitrides such as GaInNAs [2, 3] and GaInNAs(Sb) [4–6] are very promising active materials for circumventing these fundamental problems in VCSEL growth. They can be combined with the well established GaAs/AlAs Bragg mirror technology and promise emission wavelengths around 1.3 and 1.55 μm [7–14]. Furthermore, the dilute nitride materials offer important advantages in comparison to InP-based materials such as higher temperature stability [15–18], due to broad gain spectra, and higher differential gain, due to a higher carrier confinement [19, 20].

However, although important improvements especially with regard to laser device development have been achieved, there is still little known about important laser properties such as the gain mechanism and the linewidth enhancement factor α in these metastable

material systems. Insights into the gain mechanism allow further improvements of laser devices which cannot be obtained by investigation of the photoluminescence alone. Moreover, the optimization of the gain spectra towards larger gain bandwidth could lead to a further optimization of the temperature stability especially for VCSEL devices [16, 19]. This could be achieved on the basis of new effects occurring for this material class, e.g. by the controlled use of additional discrete bandgaps in GaInNAs arising from different possible nearest-neighbour configurations of the nitride N in the GaInAs matrix [21, 22].

Detailed knowledge of the linewidth enhancement factor α is important for further optimization also, because it determines the chirp of optical pulses in directly modulated lasers.

In this paper, we present experimental studies of the gain and linewidth enhancement factor α in state-of-the-art 1.3 μm GaInNAs/GaAs quantum well lasers. The paper is organized as follows. Section 2 describes the laser samples investigated. Section 3 deals with experimental techniques and details of measuring the gain and linewidth enhancement factor in semiconductor lasers. The results for GaInNAs laser devices are presented and discussed in section 4 and finally summarized in section 5.

2. Samples

The samples studied in this work are laterally single-mode ridge-waveguide (GaIn)(NAs)/GaAs laser structures. These edge emitters were grown by molecular-beam epitaxy on n-GaAs substrates and were all processed from the same wafer. A radio-frequency (RF)-coupled plasma source was used to generate reactive nitrogen from N_2. The active region contains three 6 nm wide $(Ga_{0.62}In_{0.38})(N_{0.019}As_{0.981})$ quantum wells which are separated by 20 nm wide $(Ga_{0.95}In_{0.05})(N_{0.015}As_{0.985})$ barriers. The active layers were symmetrically inserted into a 300 nm thick undoped GaAs waveguide layer. The p- and n-type cladding layers consist of 1.5 μm thick $Ga_{0.7}Al_{0.3}As$ doped with Be and Si, respectively. A highly p-doped GaAs layer was used as a contact layer [23]. The N content is determined solely by the N flux, assuming that all reactive nitrogen is completely and preferentially incorporated at growth temperatures below 520 °C [24]. The absolute uncertainty of the N content is estimated to be $\pm 0.5\%$ [16]. The thermal annealings of the nitride-containing layers were automatically performed during growth of the upper cladding and p-contact layers [24, 25]. The ridge-waveguide laser structures were processed using an Ar ion dry etching technique and RF-sputtered SiN_x [23]. The laser emission wavelength is 1.28 μm. The laser diode used for the gain measurements with the transmission method has a cavity length of 200 μm and a narrow stripe width of 3.5 μm. Both facets of this laser are antireflection coated with a single layer which leads to residual reflectivities of approximately 2% per facet. The laser diode used for the gain measurements with the method of Hakki and Paoli and for the investigation of the α-factor discussed in section 4.2 is 350 μm long and has a narrow stripe width of 4 μm. The facets are uncoated. The threshold current at room temperature in continuous wave (cw) operation of this laser sample is 19 mA. Further details about electrical properties and laser performance in pulsed and cw conditions were already published in [23].

3. Experimental details

Lots of different techniques are commonly used to measure the gain in edge emitting lasers. Examples are the method established by Henry [26, 27], the electrical or optical stripe length method [28, 29], the widely used method of Hakki and Paoli [30] and methods based on

transmission or pump–probe experiments [31]. The gain investigations presented in this paper were done by the method of Hakki and Paoli in comparison to a transmission method.

3.1. Gain measurements with the method of Hakki and Paoli

The method of Hakki and Paoli evaluates the gain from the Fabry–Perot modulation depth in the amplified spontaneous emission (ASE) spectra of an edge emitting laser below threshold. Although this technique is conceptually simple, it suffers from few limitations. It is only reasonable to measure the gain below threshold due to the clamping of the carrier density above the laser threshold. The use of antireflection coatings to increase the threshold introduces difficulties, because the wavelength dependence of the facet reflectivity has to be precisely known for the evaluation of the gain. Additionally it substantially complicates the accurate detection of the Fabry–Perot modulation due to a reduced modulation depth. Furthermore, and most important, the method requires very highly resolved measurements of the ASE spectra to push the measurement error for the gain as low as possible [32]. To check for possible errors in gain evaluation due to the limited resolution, we convoluted an ideal Fabry–Perot mode for $RG = 0.8$ with a typical, unit area, triangle response function for our optical spectrum analyser. R is the reflectivity of the facets and G the single-pass intensity gain, defined as

$$G = \mathrm{e}^{Lg}$$

where g is the single-pass net modal gain and L the cavity length. Figure 1 displays the original unmodified Fabry–Perot mode in comparison to the modes detected with 12 and 50 pm resolution. The convoluted mode for 50 pm full width at half-maximum (FWHM) already shows a strong reduction of the modulation depth in combination with a broadening of the mode. This leads to a significant underestimation of the gain. The error in gain evaluation depends on the reflectivity–gain product RG due to a change of the Fabry–Perot mode shape. Therefore not only the absolute value of the gain but also the shape of the gain spectrum changes with resolution. The reflectivity–gain product dependent behaviour of the gain evaluation error for the method of Hakki and Paoli is presented in figure 2(a). With a resolution of 12 pm it is possible to reduce the error to values less than 1%. Another possibility for circumventing these difficulties is to use the modified approach of Cassidy [33]. This method extracts the gain from the Fabry–Perot modes as well. But instead of evaluating the gain from the modulation depth and the ratio of maximum intensity to minimum intensity, as in the case of the method described before, it is calculated from the ratio of average mode intensity to minimum intensity. This approach is less sensitive to the system resolution but more sensitive to noise [32]. The error in gain evaluation for this method is shown in figure 2(b). Considering these results, we used an optical spectrum analyser (OSA) with resolution of 12 pm around 1.3 μm wavelength for our gain measurements with the method of Hakki and Paoli.

3.2. Linewidth enhancement measurements calculated from the Fabry–Perot mode shift

The measurement of highly resolved ASE spectra as required for the gain measurements with the approach of Hakki and Paoli allows one to investigate the linewidth enhancement factor α easily from nearly the same data. The α-factor is given by

$$\alpha = -\frac{4\pi}{\lambda}\left(\frac{\Delta n}{\Delta N}\Big/\frac{\Delta g}{\Delta N}\right)$$

with Δn being the refractive index change and Δg the variation of the net modal gain due to a carrier density change ΔN in the active material [34]. The net modal gain change can be determined directly using the method of Hakki and Paoli. The refractive index change Δn

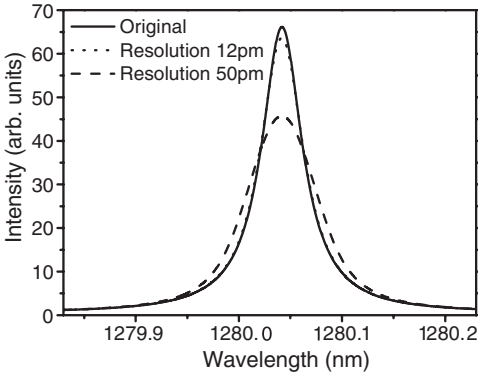

Figure 1. Typical Fabry–Perot modes for a reflectivity–gain product $RG = 0.8$. The original case (solid) and after convoluting with a spectrometer response function of 12 pm (dotted) and 50 pm FWHM (dashed).

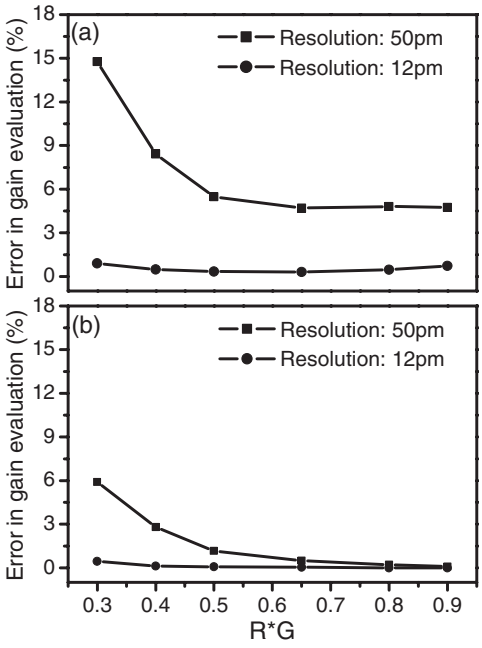

Figure 2. The error in gain evaluation for different resolutions of the optical spectrum analyser, depending on the reflectivity–gain product. (a) shows the behaviour for the method of Hakki and Paoli, while (b) shows that for the modified approach of Cassidy.

with injection current variation $\Delta\lambda$ can be calculated from the wavelength shift ΔI of the Fabry–Perot modes. Using

$$\frac{\Delta n}{\Delta I} = -\frac{n}{\lambda}\frac{\Delta\lambda}{\Delta I}$$

the α-factor can be written as [35]

$$\alpha = -\frac{4\pi n}{\lambda^2}\frac{\Delta\lambda}{\Delta g}.$$

A spectral resolution high enough for detecting the mode shift with enough accuracy is important for this approach. The α-factor data presented in this paper were measured with a resolution of 12 pm. The laser diode was operated under continuous wave conditions at room temperature. To reduce heating, we used a Peltier-based active temperature control. In spite of the temperature stabilization, a small temperature shift in the active layer, due to the varying current flow, could not be avoided. It could, in principle, be suppressed by operating the laser, pulsed, with a very small duty cycle. Combined with the requirements for spectral resolution, this leads often to difficulties due to poor signal-to-noise ratio. Our approach for accounting for the additional shift of the Fabry–Perot modes due to this residual heating is as follows.

Assuming that the heating in the active layers is dominantly due to the Ohmic resistance of the laser diode, the heating is a function of the injection current only. The heating induced mode shift can be separately investigated by taking into account that the carrier density is clamped at the threshold density for currents above threshold. Therefore the wavelength shift of the Fabry–Perot modes for current variation above threshold is only caused by heating and

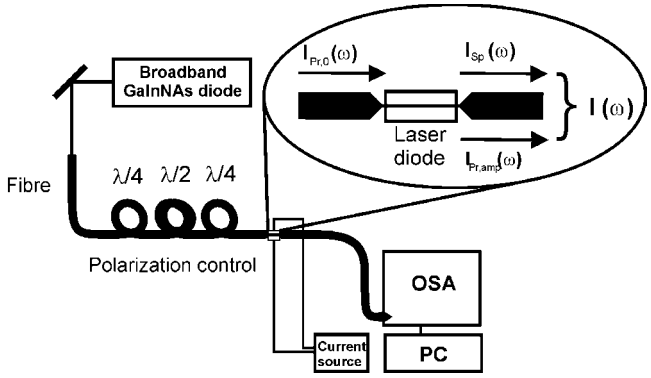

Figure 3. The experimental set-up for the transmission approach for measuring the optical gain. A GaInNAs laser diode comparable to the sample and operated below threshold was used as a broadband light source for the probe light.

contains no carrier density variation induced contributions. This behaviour above threshold can be extrapolated to currents below threshold to extract the pure carrier density induced shift [36, 37]. Our α-factor results were corrected by this approach.

3.3. Gain measurements with a transmission method

Even though the resolution requirements can be satisfied, the approach of Hakki and Paoli is only able to give spectral information about the gain over a limited spectral region around the gain peak. It is not possible to measure in spectral regions with stronger absorption due to the lack of ASE intensity. In order to circumvent these restrictions we additionally use a gain measurement technique based on a transmission approach developed by Ellmers *et al* [31]. This transmission method is a powerful alternative experimental technique for determining the gain over a very broad spectral range far down into the absorption region with very high quantitative precision. The experimental set-up is shown schematically in figure 3. The broadband light source used to probe directly the single-pass gain of the GaInNAs laser diode is a superluminescence diode, which is almost identical to the sample under study. To measure the gain, the probe light is coupled into a single-mode fibre and then from the fibre into the waveguide of the sample using fibre microlenses. The light intensities propagating from one laser to the other are small enough to inhibit significant interaction among them. The polarization of the probe light can be controlled using fibre loops in order to measure polarization dependent gain for the transverse electric (TE) and the transverse magnetic (TM) mode. The sample and the probe light source are pumped electrically with low noise current sources. The light output from the sample is coupled into a fibre as well and detected with an OSA. The ASE spectra of the sample with, $I(\omega)$, and without probe light, $I_{\mathrm{sp}}(\omega)$, are measured as well as the probe spectrum of the broadband light source $I_{\mathrm{pr},0}(\omega)$. The gain can be extracted from these spectra using [38]

$$g(\omega) = \frac{1}{L} \ln \left(\frac{I(\omega) - I_{\mathrm{sp}}(\omega)}{I_{\mathrm{pr},0}(\omega)} \right)$$

where $g(\omega)$ is the single-pass net modal gain and L the cavity length. This holds only in the linear regime, i.e. the probe intensity has to be low. Moreover, this concept assumes a single-pass propagation of the probe light through the sample. To ensure this, the sample has to be coated on both facets with antireflection layers which requires additional processing steps and

represents a relevant restriction of this approach. Furthermore, the value of the probe power coupled into the waveguide is difficult to measure precisely. Assuming constant coupling over the entire wavelength range, this uncertainty introduces a constant offset to the gain spectra. The offset can be extracted from the data in the transparency region at lower photon energies. Anyway, it is not possible to measure waveguide losses with this approach in contrast to the method of Hakki and Paoli.

3.4. Calculation of the linewidth enhancement factor using Kramers–Kronig relations

As discussed in section 3.2 the linewidth enhancement factor α describes the ratio of the refractive index change to the variation of the gain due to a change of the carrier density and therefore describes the ratio of the variations of the real and imaginary parts of the complex refractive index. In linear systems the relationship of the real and imaginary parts of the complex refractive index can be described by the Kramers–Kronig relations [39]. This allows one to calculate the spectral dependence of the refractive index change Δn, if the change in absorption $\Delta\alpha$ or gain $\Delta g = -\Delta\alpha$ is known, using

$$\Delta n(\omega) = \frac{c}{\pi} P \int_{\omega_2}^{\omega_1} \frac{\Delta\alpha(\omega')}{(\omega')^2 - \omega^2}\, \mathrm{d}\omega'$$

where P is the principal value of the integral and $\omega_2 \rightarrow \omega_1$ is the spectral range, where the absorption change is non-negligible [40]. The transformation from Δg to Δn is only accurate if Δg is known over the whole spectral range where it is non-negligible. However, the contributions of Δg at frequencies ω', affecting the calculation of Δn at frequencies ω, are normalized with $\frac{1}{(\omega')^2-\omega^2}$. Therefore the influences are decreasing with increasing spectral distance but are not negligible, anyway. Since the transmission method provides the gain and the differential gain over a very broad spectral range, one might speculate on whether the Δg spectra are sufficient for calculating reliable Δn spectra and α-factor spectra using the Kramers–Kronig transformation. However, the detailed discussion in section 4.4 will show that even the knowledge of the differential gain over a 275 meV wide spectral range around the emission wavelength is insufficient for getting more than qualitative information about the linewidth enhancement factor.

4. Results and discussion

4.1. Gain measurements with the method of Hakki and Paoli

Figure 4 presents gain spectra for different injection currents from 5.7 to 17.2 mA and 0.3 to 0.9 times threshold, measured by the method of Hakki and Paoli. The measurements were done at room temperature under continuous wave operation. The peak of the net modal gain spectrum for 0.9 times threshold is at 1280 nm and has the value of 25.8 cm^{-1}. The full width at half-maximum for this spectrum is 33 meV. The waveguide losses for this structure can be determined from the transparency region of the gain spectra as 2 cm^{-1}. The spectra are not polarization resolved and therefore, in principle, include contributions from TE and TM polarized gain. However, results discussed later show that the gain contains only marginal TM contributions.

It was shown recently [41] that these gain spectra are very similar to those for commercial 1.3 μm InP-based laser structures. This shows that the active material is competitive for applications and gives rise to the assumption that the laser process is similar to that in the well established material system. This will be addressed further in section 4.3.

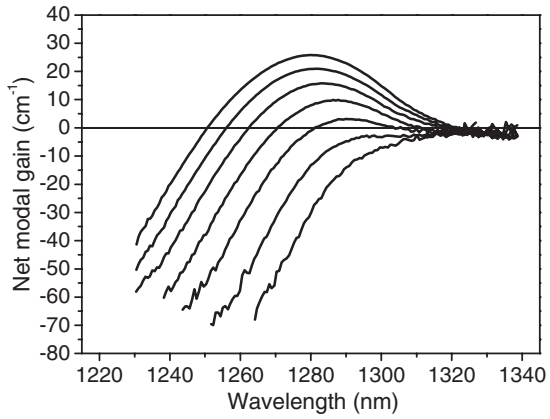

Figure 4. Experimental gain spectra for a GaInNAs laser, measured by the method of Hakki and Paoli for injection currents of 5.7, 7.6, 9.6, 11.5, 13.4, 15.3 and 17.2 mA.

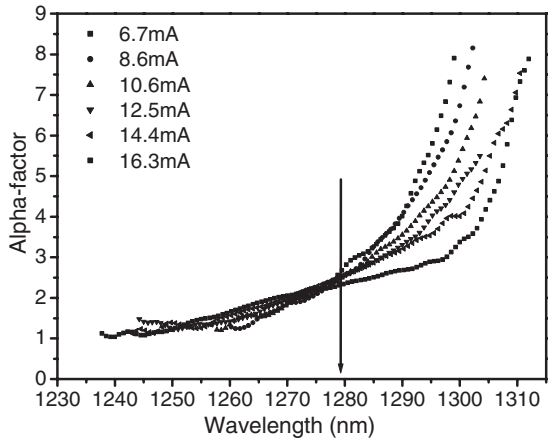

Figure 5. Experimental spectra of the linewidth enhancement factor for a GaInNAs laser for different injection currents of 6.7, 8.6, 10.6, 12.5, 14.4 and 16.3 mA. The spectra were obtained by analysing the Fabry–Perot modes with carrier density variation. The laser emission wavelength at threshold is marked by an arrow.

4.2. Linewidth enhancement measurements calculated from the Fabry–Perot mode shift

Using the method for determining the refractive index change described in section 3.2 in combination with the gain results shown in figure 4 we were able to investigate the linewidth enhancement factor of the GaInNAs laser diode with good accuracy. The uncertainty in the amplitude of α is ± 0.4. The results for current windows around 6.7–16.3 mA or 0.35–0.85 times threshold are displayed in figure 5. The laser emission wavelength at threshold is marked by an arrow. The value of α at this fixed wavelength is around 2.5 ± 0.4 and almost constant with variation of the carrier density and current, as presented in figure 6: α varies by less than 0.35 for currents between 6.7 and 16.3 mA. This clamping behaviour of α for fixed wavelength observed in these GaInNAs lasers can be an important feature for VCSELs. In contrast to edge emitting lasers, where the emission wavelength follows the gain peak with variation of the current, the emission wavelength in VCSELs remains constant because it is set by the cavity mode. Thus, a small variation of the linewidth enhancement factor at a fixed wavelength is crucial for the VCSEL optimization. The clamping behaviour investigated and the spectral dependence of α agree very well with results obtained from a microscopic theory based on the kp method and using the anticrossing model as developed for GaInNAs [37, 43–45].

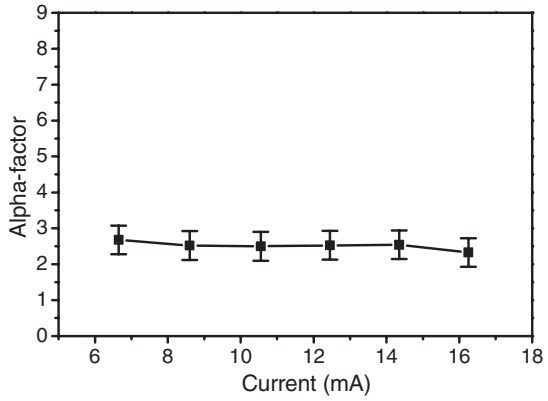

Figure 6. The clamping behaviour of the linewidth enhancement factor at the laser emission wavelength. The α-factor is around 2.5 and almost constant over a broad carrier density range.

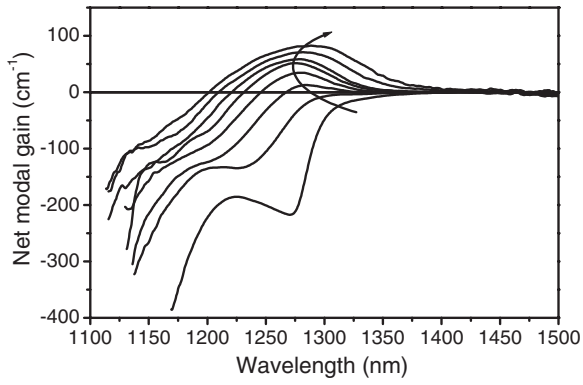

Figure 7. Experimental gain spectra for a GaInNAs laser, measured by the transmission method for injection currents of 0, 5, 10, 15, 20, 30, 50 and 70 mA. The additional red-shift is due to device heating at higher currents.

4.3. Gain measurements with a transmission method

The experimental techniques based on the analysis of the Fabry–Perot modes produce accurate results as regards gain and linewidth enhancement factor over a spectral region of approximately 75 meV around the gain peak and for carrier densities below threshold. However, to obtain further insight into the material system and to determine the laser process unambiguously, it is necessary to get more spectral and carrier density dependent information on the gain. This is possible with the transmission method presented in section 3.3. Gain spectra for TE polarized light, measured with the transmission method for different currents from 0 to 70 mA, are displayed in figure 7. The spectra were measured at room temperature in continuous wave operation without active temperature control. Accordingly, the spectra show an additional red-shift due to heating at higher currents in addition to the normal blue-shift of the gain peak with increasing carrier density.

The current values corresponds to approximately 0 to 5 times the original threshold without antireflection coatings. Therefore the transmission method allows the determination of the gain over a much larger carrier density range especially far down into the absorption region and for zero injection current. The excitonic dip at 1271 nm, clearly visible at zero injection current, marks the dominant quantum well transition. The dip is disappearing with increasing current and at 70 mA gain can be observed with a peak value of 83 cm^{-1} and a full width at half-maximum of 83 meV.

Apart from the larger carrier density range, the transmission method produces much more spectral information. A comparison between the transmission method and the method of Hakki

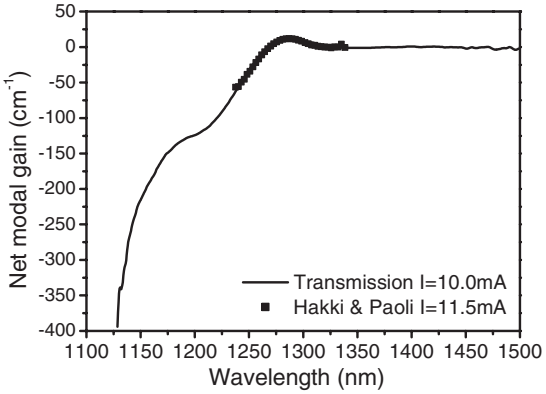

Figure 8. Comparison of gain spectra measured by the method of Hakki and Paoli (symbols) and the transmission method (curve). The transmission method allows one to determine the gain over a much larger spectral range.

and Paoli is presented in figure 8 and confirms this conclusion. The gain spectrum determined with the transmission method is approximately 275 meV wide in contrast to 75 meV for the method of Hakki and Paoli. The high quantitative precision and the large information content of the spectra obtained from the transmission method provide a perfect basis for a comparison with a microscopic theory in order to analyse details of the laser process in the material. The experimental gain spectra of this GaInNAs laser can be described very well by a fully microscopic theory based on inhomogeneously broadened band–band transitions [37]. We conclude from the very good agreement between experiment and theory that the gain in this MBE-grown GaInNAs laser can be fully described by inhomogeneously broadened band–band transitions. High density quantum dots as reported for the metastable GaInNAs system [42] by another group are not relevant for our MBE-grown and annealed structure. However, the strong inhomogeneous broadening is not yet fully understood. Possible explanations could span from fluctuations in quantum well thickness or material composition to contributions of nearest-neighbour configuration fluctuations of N in the GaInAs matrix [16, 21, 22].

The larger amount of spectral information obtained with the transmission method can be further used to get even more insight into the quantum well transitions relevant for the gain in this GaInNAs laser structure. Figure 9 displays a comparison between TE polarized (a) and TM polarized (b) gain which shows strong differences. While for TE gain we measured large positive gain for 35 mA at 1280 nm and a strong absorption dip for zero injection current, only marginal gain and absorption changes at this wavelength could be found for TM gain. This can be explained by the compressive strain of the GaInNAs quantum wells which leads to a strong heavy-hole (hh)–light-hole (lh) splitting. The gain is dominantly generated by the confined heavy-hole-1–electron-1 transition which is only contributing to the TE polarized gain. The TM polarized gain spectra show no region with positive gain due to the fact that the lh is not confined in the quantum well due to the large hh–lh splitting [46]. Therefore the light-hole transitions contribute only very weakly to the gain spectra.

4.4. Calculation of the linewidth enhancement factor using Kramers–Kronig relations

As discussed in section 3.4, knowledge of the differential gain spectrum over a sufficiently broad spectral range allows the calculation of the refractive index change and therefore the determination of the linewidth enhancement factor. The differential gain spectrum obtained by the transmission method for 12.5 mA (current window 5 mA) is plotted in figure 10(a). Even with the transmission method the spectra are not accessible at energies above 1.1 eV (1130 nm) due to the strong absorption. Unfortunately, this is also the region with the largest differential

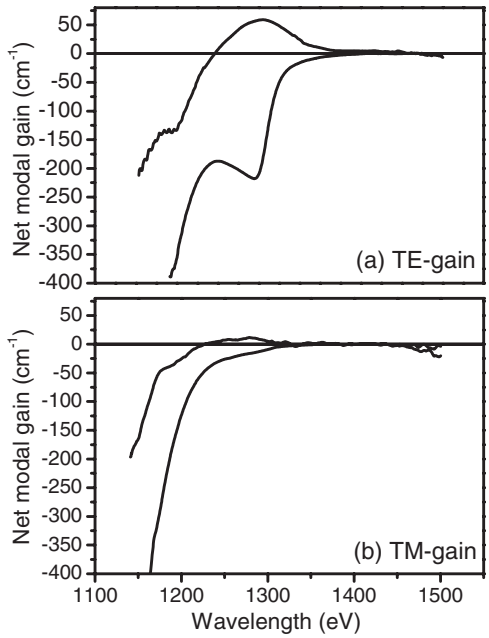

Figure 9. Comparison of the optical gain of a GaInNAs laser diode for TE polarization (a) and TM polarization (b). The injection currents were 0 and 35 mA. The polarization resolved gain spectra were measured by the transmission method. The TM gain contributes only marginally due to unconfined light-hole states.

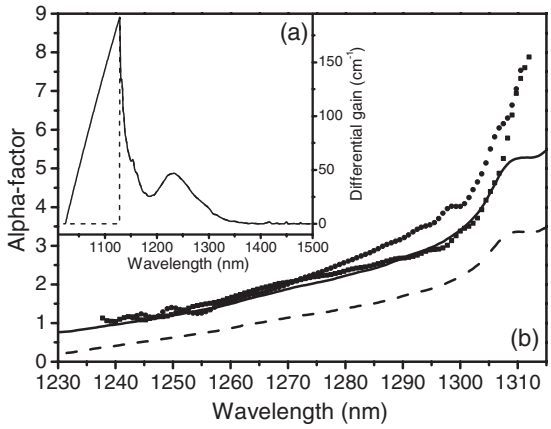

Figure 10. The differential gain spectrum for a current window around 12.5 mA measured by the transmission method (a). Two different extrapolations for differential gain contributions at higher energies were used to calculate the linewidth enhancement factor using Kramers–Kronig relations ((a), solid curve, dashed line). (b) shows the calculated results for both extrapolations (curves) in comparison with results measured by the method described in section 3.2 with a comparable sample (symbols) for injection currents 14.4 (circles) and 16.3 mA (squares).

gain. To evaluate whether these contributions of the differential gain at higher energies are relevant for the determination of the α-factor around the laser emission wavelength we used two extremely different extrapolations of the differential gain spectra. The first one sets the differential gain to zero for higher energies. The second one assumes a linear decrease in contribution with increasing energy, as displayed in figure 10(a). This concept of extrapolating the differential gain spectra is only reliable if both extrapolations would provide the same value for α at the laser emission wavelength. For GaAlAs bulk laser structures this concept was reported to be successful [47]. The calculated α-factor spectra for both extrapolations

are plotted in figure 10(b), in comparison to results obtained by the method based on Fabry–Perot mode analysis. The spectral behaviours for the two extrapolations are quite similar and are comparable to the results obtained by the Fabry–Perot method. But the absolute values of α differ considerably for the different high energy extrapolations of the differential gain. Obviously, the variation of the absorption at high energies due to varying carrier densities in the barrier states is of great relevance for the refractive index and thus for the α-factor of our GaInNAs structure. Therefore the technique for calculating the α-factor from the gain results measured by the transmission method, though providing qualitative information about the spectral behaviour of the α-factor, is insufficient for determining absolute values for α for GaInNAs/GaAs QW structures.

5. Conclusions and outlook

In conclusion, we have extensively analysed the gain and α-factor spectra of a state-of-the-art 1.3 μm GaInNAs laser structure using two experimental concepts: the evaluation of the Fabry–Perot modes in the amplified spontaneous emission spectra (the method of Hakki and Paoli) and the transmission method with a broadband probe. The Hakki–Paoli measurements provided gain spectra over a limited spectral region and reliable spectra for the α-factor. The transmission method, in contrast, provides quantitative gain spectra over a large spectral range and over a large range of carrier densities. The approach for extracting the α-factor via a Kramers–Kronig transformation failed because the differential gain spectra were still incomplete.

We find that the gain spectra of our GaInNAs structure are similar to those of commercial InP-based structures and conclude that the material is competitive for telecommunication applications at 1.3 μm. The linewidth enhancement factor has a typical value of 2.5 at the laser emission wavelength and clamps at this value for increasing injection current.

The optical gain in our material arises from inhomogeneously broadened band–band transitions. However, the origin of the inhomogeneous broadening has yet to be exactly determined. Moreover, other groups have reported high density quantum dot behaviour for GaInNAs material [42] and we have found strong indications that the gain mechanism in MOCVD-grown material without intentional annealing is considerably different from that for the MBE-grown annealed structures analysed here [21]. Using gain measurements with the stripe length method, we obtained structured gain spectra due to locally varying environments of the nitrogen in the lattice [19].

This substantial variation of the observations for structures fabricated under different conditions shows that there is a large potential for intentionally designing the optical properties of the metastable dilute nitrides, which should be further exploited in the future.

Acknowledgments

The GaInNAs samples were provided by A Y Egorov, B Borchert and H Riechert from Infineon Technologies. Parts of this work were supported by the Bundesministerium für Bildung, Wissenschaft, Forschung und Technologie (BMBF) and Infineon Technologies. We would like to thank J Hader, J V Moloney and S W Koch for support with their microscopic theory and for fruitful discussions, and G Weiser for providing the program for the Kramers–Kronig transformation. We also thank W W Rühle for experimental support and helpful discussions.

References

[1] Hansmann S, Walter H, Hillmer H and Burkhard H 1994 *IEEE J. Quantum Electron.* **30** 2477
[2] Kondow M, Uomi K, Niwa A, Kitatani T, Watahiki S and Yazawa Y 1996 *Japan. J. Appl. Phys.* **35** 1273
[3] Höhnsdorf F, Koch J, Agert C and Stolz W 1998 *J. Cryst. Growth* **195** 391

[4] Shimizu H, Kumada K, Uchiyama S and Kasukawa A 2000 *Electron. Lett.* **36** 1701
[5] Ha W N, Gambin V, Bank S, Wistey M, Yuen H, Kim S and Harris J S 2002 *IEEE J. Quantum Electron.* **38** 1260
[6] Bank S, Ha W, Gambin V, Wistey M, Yuen H, Goddard L, Kim S and Harris J S 2003 *J. Cryst. Growth* **251** 367
[7] Ellmers C, Höhnsdorf F, Koch J, Agert C, Leu S, Karaiskaj D, Hofmann M, Stolz W and Rühle W W 1999 *Appl. Phys. Lett.* **74** 2271
[8] Choquette K D, Klem J F, Fischer A J, Blum O, Allerman A A, Fritz I J, Kurtz S R, Breiland W G, Sieg R, Geib K M, Scott J W and Naone R L 2000 *Electron. Lett.* **36** 1388
[9] Steinle G, Egorov A Y and Riechert H 2001 *Electron. Lett.* **37** 93
[10] Sato S, Nishisyama N, Miyamoto T, Takahashi T, Jikutani N, Arai M, Matsutani A, Koyama F and Iga N 2000 *Electron. Lett.* **36** 2018
[11] Riechert H, Ramakrishnan A and Steinle G 2002 *Semicond. Sci. Technol.* **17** 892
[12] Ramakrishnan A, Steinle G, Degen C and Ebbinghaus G 2002 *Electron. Lett.* **38** 322
[13] Gollub D, Fischer M and Forchel A 2002 *Electron. Lett.* **38** 1183
[14] Fischer M, Gollub D, Reinhardt M, Kamp M and Forchel A 2003 *J. Cryst. Growth* **251** 1
[15] Wagner A, Ellmers C, Höhnsdorf F, Koch J, Agert C, Leu S, Hofmann M, Stolz W and Rühle W W 2000 *Appl. Phys. Lett.* **76** 271
[16] Hofmann M R, Gerhardt N, Wagner A, Ellmers C, Höhnsdorf F, Koch J, Stolz W, Koch S W, Rühle W W, Hader J, Moloney J V, O'Reilly E P, Borchert B, Egorov A Y, Riechert H, Schneider H C and Chow W W 2002 *IEEE J. Quantum Electron.* **38** 213
[17] Kitatani T, Nakahara K, Kondow M, Uomi K and Tanaka T 2000 *Japan. J. Appl. Phys.* **39** L86
[18] Kondow M, Kitatani T, Nakahara K and Tanaka T 2000 *IEEE Photon. Technol. Lett.* **12** 777
[19] Gerhardt N, Hofmann M R and Rühle W W 2003 *IEE Proc., Optoelectron.* **150** 45
[20] Hader J, Moloney J V, O'Reilly E P, Hofmann M R and Koch S W 2001 *Proc. SPIE* **4283** 36
[21] Choulis S A, Hosea T J, Klar P J, Hofmann M and Stolz W 2001 *Appl. Phys. Lett.* **79** 4277
[22] Klar P J, Grüning H, Koch J, Schäfer S, Volz K, Stolz W, Heimbrodt W, Kamal Saadi A M, Lindsay A and O'Reilly E P 2001 *Phys. Rev.* B **64** 121203
[23] Borchert B, Egorov A Y, Illek S, Komainda M and Riechert H 1999 *Electron. Lett.* **35** 2204
[24] Riechert H, Egorov A Y, Livshits D, Borchert B and Illek S 2000 *Nanotechnology* **11** 201
[25] Borchert B, Egorov A Y, Illek S and Riechert H 2000 *IEEE Photon. Technol. Lett.* **12** 597
[26] Henry C, Logan R and Merritt K 1980 *J. Appl. Phys.* **51** 3042
[27] Blood P, Kucharska A, Jacobs J and Griffiths K 1991 *J. Appl. Phys.* **70** 1144
[28] Thomson J D, Summers H D, Hulyer P J, Smowton P M and Blood P 1999 *Appl. Phys. Lett.* **75** 2527
[29] Hvam J 1978 *J. Appl. Phys.* **49** 3124
[30] Hakki B W and Paoli T L 1975 *J. Appl. Phys.* **46** 1299
[31] Ellmers C, Hofmann M, Rühle W W, Girndt A, Jahnke F, Chow W W, Knorr A, Koch S W, Hanke C, Korte L and Hoyler C 1998 *Appl. Phys. Lett.* **72** 1647
[32] Jordan V 1994 *IEE Proc., Optoelectron.* **141** 13
[33] Cassidy D T 1984 *J. Appl. Phys.* **56** 3096
[34] Osinski M and Buus J 1987 *IEEE J. Quantum Electron.* **23** 9
[35] Newell T C, Bossert D J, Stintz A, Fuchs B, Malloy K J and Lester L F 1999 *IEEE Photon. Technol. Lett.* **11** 1527
[36] Zhao B, Chen T R, Wu S, Zhuang Y H, Yamada Y and Yariv A 1993 *Appl. Phys. Lett.* **62** 1591
[37] Gerhardt N C, Hofmann M R, Hader J, Moloney J V, Koch S W and Riechert H 2004 *Appl. Phys. Lett.* **84** 1
[38] Hofmann M R 1999 *Recent Res. Dev. Appl. Phys.* **2** 269
[39] Yu P Y and Cardona M 1999 *Fundamentals of Semiconductors* 2nd edn (Berlin: Springer) p 240
[40] Fleming S C and Whitley T J 1996 *IEEE J. Quantum Electron.* **32** 1113
[41] Hofmann M, Wagner A, Ellmers C, Schlichenmeier S, Schäfer S, Höhnsdorf F, Koch J, Leu S, Stolz W, Koch S W, Rühle W W, Hader J, Moloney J V, O'Reilly E P, Borchert B, Egorov A Yu and Riechert H 2001 *Appl. Phys. Lett.* **78** 3009
[42] Xin H P, Kavanagh K L, Zhu Z Q and Tu C W 1999 *Appl. Phys. Lett.* **74** 2337
[43] Shan W, Walukiewicz W, Ager J W II, Haller E E, Geisz J F, Friedman D J, Olson J M and Kurtz S R 1999 *Phys. Rev. Lett.* **82** 1221
[44] O'Reilly E P and Lindsay A 1999 *Phys. Status Solidi* b **216** 131
[45] Hader J, Moloney J V, Koch S W and Chow W W 2003 *IEEE J. Sel. Top. Quantum Electron.* **9** 688
[46] Chow W W, Jones E D, Modine N, Allerman A and Kurtz S 1999 *Appl. Phys. Lett.* **75** 2891
[47] Hofmann M, Koch M, Heinrich H-J, Weiser G, Feldmann J, Elsäßer W, Göbel E O, Chow W W and Koch S W 1994 *IEE Proc., Optoelectron.* **141** 127